J Appl Electrochem (2009) 39:791–798
DOI 10.1007/s10800-008-9723-z

ORIGINAL PAPER

Time averaged temperature calculations in pulse electrochemical machining, spectral approach

N. Smets · S. Van Damme · D. De Wilde · G. Weyns · J. Deconinck

Received: 16 September 2008 / Accepted: 6 November 2008 / Published online: 25 November 2008

Abstract Simulation of the temperature distribution during the Pulse Electrochemical Machining (PECM) process provides information on system design and guidelines for practical use. The pulses that are applied to the PECM system have to be described on a time scale that can be orders of magnitude smaller than the time scale on which the thermal effects evolve. If the full detail of the applied pulses has to be taken into account, the time accurate calculation of the temperature distribution in PECM can become a computationally very expensive procedure. A different approach is used by time averaging the heat sources of the system. Performing this, the time steps used during the calculations are no longer dictated by the pulse characteristics. Using this approach, computationally very cheap, yet satisfying results can be obtained. In previous work of the authors, the hybrid calculation and the Quasi Steady State ShortCut (QSSSC) were introduced. This method allows to perform simplified calculations while getting satisfactory results. The method introduces errors however, which were quantified using analytical solutions and found to be acceptable. The results applied only to rectangular pulses. In this work, the more general case of arbitrary pulse forms is considered using a spectral approach.

Keywords Pulse electrochemical machining · Temperature distribution · Time averaging · Transient · Spectral approach

N. Smets (✉) · S. Van Damme · D. De Wilde · G. Weyns · J. Deconinck
IR/ETEC Department, Vrije Universiteit Brussel, Pleinlaan 2, 1050 Brussels, Belgium
e-mail: nsmets@vub.ac.be

Abbreviations

1D	One dimensional
ECM	Electrochemical machining
PECM	Pulse electrochemical machining
QSS	Quasi steady state
QSSSC	Quasi steady state shortcut
SS	Steady state

List of symbols

A	Pulse scale factor (K)
Bi	Biot number $(=\frac{hH}{k})(-)$
C_p	Heat capacity (J kg^{-1} K^{-1})
Fo	Fourier number $(=\frac{\alpha' t}{H^2})(-)$
h	Heat transfer coefficient (W m^{-2} K^{-1})
H	Characteristic size electrode (m)
J	Current density (A m^{-2})
k	Thermal conductivity (W m^{-1} K^{-1})
n	Spectral component index (–)
P_{dl}	Heat density produced in the double layer (W m^{-2})
P_{bulk}	Heat density produced in the bulk (W m^{-3})
t	Time (s)
t'	Time (s)
T	Pulse period (s)
T'	Dimensionless pulse period (–)
v	Scalar velocity (m s^{-1})
$\overline{v}$	Velocity vector (m s^{-1})
x	Distance (m)
x'	Dimensionless distance (–)
α	Duty cycle (–)
α'	Thermal diffusivity (m^2 s^{-1})
η	Overpotential (V)
θ	Relative temperature (K)
$\overline{\theta}$	Averaged temperature (K)
$\tilde{\theta}$	Temperature ripple (K)

θ_{decay}	Decaying temperature (K)
Θ	Temperature (K)
Θ_∞	Reference temperature (K)
Θ^*	Electrolyte temperature (K)
$\hat{\lambda}_n$	Transcendental coefficients (–)
ρ	Density (kg m^{-3})
σ	Electrical conductivity (S m^{-1})
τ	Time constant (s)
ω	Angular frequency (s^{-1})
ψ	Pulse delay (s)

1 Introduction

Electrochemical Machining (ECM) is a manufacturing process based on the controlled anodic dissolution of a metal at large current densities (in the range of 1 A mm^{-2}). An electrolyte is used to carry away produced heat, among other reaction products.

Despite its advantages, some difficulties still trouble the application of ECM. One important issue is the lack of quantitative simulation software to predict the tool shape and machining parameters necessary to produce a given work-piece profile [1–3]. The most complete model needs to deal with the effects of the fluid flow, gas evolution, heat generation, the electrochemical processes at the electrodes, the transport of the species involved and all this while the electrode shape changes. The work reported below makes a contribution in incorporating heat generation in the model, and calculating the temperature distributions.

Pulse Electrochemical Machining (PECM) involves the application of current or voltage pulses. One wishes to apply pulses for reasons of accuracy and surface quality [3–6]. The issue of heating of the electrolyte is of primary importance for the determination of the limiting conditions in ECM [5–9].

Steady State (SS) temperature distribution calculations have been performed by Clark [8], Loutrel [9] and Kozak [7]. Time accurate calculations of temperature distribution during PECM have already been performed by Kozak [4, 5]. In [4, 5], the pulses are considered to be independent of each other, and thus no accumulation of heat over multiple periods is encountered. Cases where there was accumulation of heat in the system during multiple pulses, have been performed in previous work of the authors [10]. It was shown that, in order to determine in advance whether the heat produced during multiple pulses is going to accumulate or not, the time scales present in the system have to be studied.

To simulate electrochemical processes with current pulses, one has to perform calculations with boundary conditions that vary in time. By applying a time stepping algorithm, all the variable distributions are calculated in time. The applied pulses have to be described on a time scale that can be orders of magnitude smaller than the time scale on which the thermal effects evolve. This means that a lot of timesteps would have to be calculated to perform a satisfactory thermal simulation, which would be a computationally very expensive procedure.

By averaging the heat production in the system, it is possible to calculate temperature evolutions with timesteps that are not dictated by the time scale of the pulses. It also provides the possibility of calculating a SS. However, plain averaging is inadequate in the system under consideration, because of the very broad spectrum of possible time scales present (see also [10]). While averaging might be necessary to handle the largest time scales, the smaller time scales may still be very important relative to the pulse period. Plain averaging would eliminate all the small time scale effects, which would make it impossible to perform accurate simulations.

To solve this problem the hybrid calculation was introduced in previous work of the authors [11]. The hybrid calculation is a method where initially averaged heat sources are applied, and at the time of interest, pulsed heat sources are applied. The QSSSC—a special case of the hybrid calculation—consists of using the averaged SS as a starting state, and applying pulses afterwards. The hybrid calculation, which is an approximative method, introduces errors in the solution. It was shown for rectangular pulses that this error is always of acceptable magnitude when the necessary measures are taken [11].

During actual numerical calculations, it is necessary to calculate far enough to judge wether the approximative method is satisfactory. To avoid these unnecessary calculations, the knowledge obtained in this paper is very useful. Numerical calculations using the hybrid technique were performed in [12] for rectangular pulses.

In this work the hybrid method is studied while applying arbitrary pulse shapes. A general formulation is made, which applies for any possible pulse shape. Two specific pulse shapes are considered for further investigations: a full-wave rectified sine and a half-wave rectified sine, see Fig. 1a and b. The externally applied voltage or current pulses will result in heat pulses in the double layers and in the electrolyte bulk. Due to the nonlinear relations the heat pulse shapes will change a little bit and hence a slightly different spectrum will be obtained. This distortion is however too complex to be considered under general circumstances, and is neglected.

The measures which have to be taken to reduce the error made with the approximative hybrid method, is by delaying the applied pulses in an intelligent way, by a certain amount ψ. For the two considered pulse shapes, analytical formulae for optimal values of ψ are presented in this

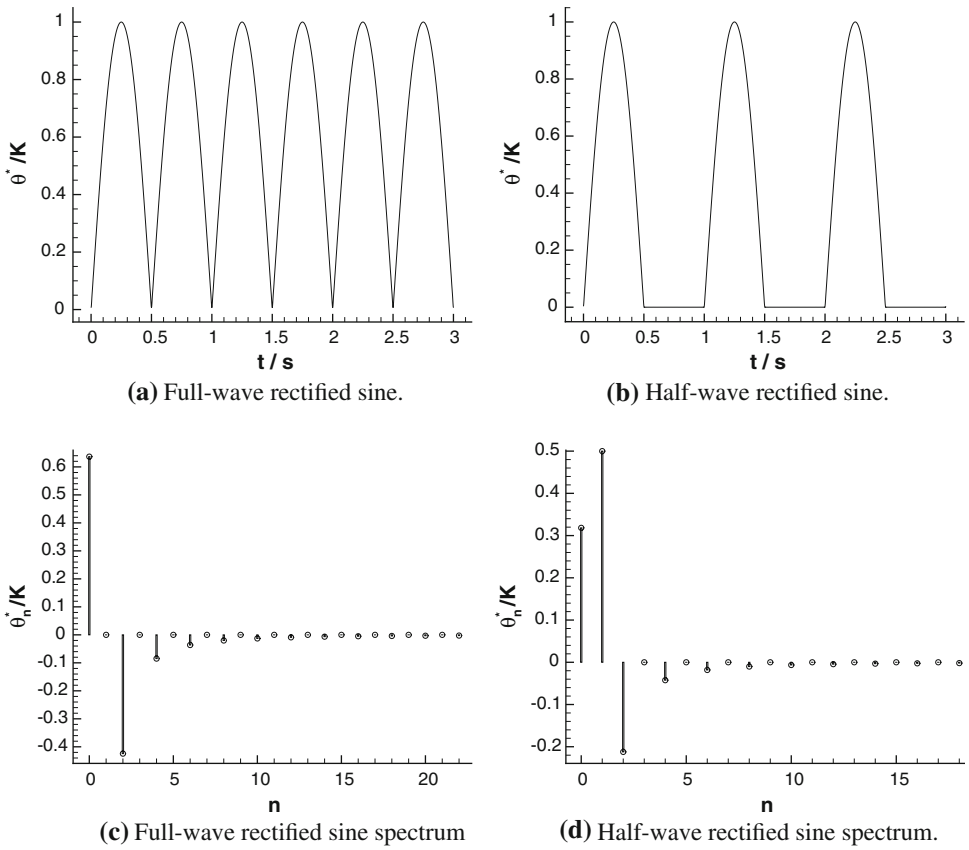

Fig. 1 Pulse shapes and their spectra. ($A = 1$ K)

(a) Full-wave rectified sine. **(b)** Half-wave rectified sine.

(c) Full-wave rectified sine spectrum **(d)** Half-wave rectified sine spectrum.

work. Also, a function E is defined to quantify how well the QSS is approximated, by using the QSSSC.

2 Mathematical model

The temperature distribution in the system is calculated using a convection-diffusion equation with heat sources:

$$\rho C_p \frac{\partial \Theta}{\partial t} + \rho C_p \overline{v} \cdot \overline{\nabla} \Theta = \overline{\nabla} \cdot \left(k \overline{\nabla} \Theta \right) + P_{bulk}. \quad (1)$$

Joule heating in the bulk of both the electrolyte and the electrodes is considered, where

$$P_{bulk} = \frac{J^2}{\sigma}. \quad (2)$$

Heat dissipation in the double layer, where [9]

$$P_{dl} = \eta J, \quad (3)$$

is also taken into account. P_{dl} is imposed as a heat flux at the electrode surfaces that are the boundaries of two domains: the electrodes and the electrolyte. The electrodes are cooled by convection. The boundaries of the electrodes, which are not contiguous to the electrolyte, are considered thermal insulators. This choice is justified by the fact that essentially all of the heat generated in the system must be carried away by the electrolyte [9].

3 Analytical solutions of simplified problems

Instead of solving Eq. 1 numerically for specific cases, an analytical approach will be performed to obtain very general results. Interesting conclusions will be drawn here, which will be extrapolated to the numerically solved case. Two subsystems are considered: conduction in the electrode, and convection in the electrolyte.

3.1 Transient conduction in a 1D slab

One electrode is considered in this system. Heat density $P_{dl}(t)$ will be produced at the contact surface with the electrolyte. Heat production in the electrode will be neglected, because of the typically very high electrical conductivity of the metal electrodes, and hence the very low heat production. The electrode is cooled by convection. The temperature distribution will be considered in one dimension only (1D).

Part of the produced heat $P_{dl}(t)$ will be removed by the electrolyte, and the other part will heat up the electrode. It was shown in [11] that the system, in which there is convective cooling into a medium at temperature Θ_∞ with a heat transfer coefficient h and simultaneous heating $P_{dl}(t)$ at the interface, is actually equivalent to the same system being heated by convection by a

medium at temperature $\Theta^*(t) = P_{dl}(t)/h + \Theta_\infty$. The latter situation will be considered in the rest of this work for easier formulation.

From the absolute temperature Θ, the relative temperature θ can be derived, using

$$\theta(t) = \Theta(t) - \Theta_\infty. \tag{4}$$

Starting from the side of the electrode which is insulated, the distance x is measured.

Using the simplifications mentioned above, Eq. 1 simplifies to

$$\frac{\partial\theta}{\partial t} = \alpha' \frac{\partial^2\theta}{\partial x^2}. \tag{5}$$

An arbitrary pulse shape can be written by means of a Fourier series. Hence the electrolyte temperature evolution will be written as

$$\theta^*(t) = \sum_{n=0}^{\infty} \theta_n^* \cos(n\omega t + \phi_n), \tag{6}$$

where θ_n^* and ϕ_n can be calculated when the pulse shape is defined, and where

$$\omega = \frac{2\pi}{T}. \tag{7}$$

The spectrum for a full-wave rectified sine is:

$$\begin{cases} \theta_0^* = \frac{2A}{\pi} & \\ \theta_1^* = 0 & \\ \theta_n^* = \frac{2A}{\pi}\frac{(-1)^n+1}{1-n^2} & n = 2,3,4,\ldots \\ \phi_n = 0 & n = 0,1,2,\ldots \end{cases} \tag{8}$$

The spectrum for a half-wave rectified sine is:

$$\begin{cases} \theta_0^* = \frac{A}{\pi} & \\ \theta_1^* = \frac{A}{2} & \\ \theta_n^* = A\frac{(-1)^n+1}{\pi(1-n^2)} & n = 2,3,4,\ldots \\ \phi_n = 0 & n = 0,2,3,\ldots \\ \phi_1 = -\frac{\pi}{2} & \end{cases} \tag{9}$$

The spectrum of a rectangular pulse is:

$$\begin{cases} \theta_0^* = A\alpha & \\ \theta_n^* = \frac{2A}{\pi n}\lvert\sin(\alpha\pi n)\rvert & n = 1,2,3,\ldots \\ \phi_0 = 0 & \\ \phi_n = \operatorname{atan2}(-1, \tan^{-1}(\alpha\pi n)) & n = 1,2,3,\ldots \end{cases} \tag{10}$$

The atan2(y, x) function computes the principal value of the arc tangent of y/x, using the signs of both arguments to determine the quadrant of the return value.

The temperature evolution in the 1D slab is then (based on the result from [13])

$$\theta(x,t) = \overline{\theta}(x,t) + \tilde{\theta}(x,t) + \theta_{decay}(x,t), \tag{11}$$

where the averaged component $\overline{\theta}(x,t)$ is

$$\overline{\theta}(x,t) = \theta_0^* \sum_{k=1}^{\infty} \beta_k(x)(1 - e^{-t/\tau_k}), \tag{12}$$

the ripple $\tilde{\theta}(x,t)$ (with zero average) is

$$\tilde{\theta}(x,t) = \sum_{n=1}^{\infty} \theta_n^* Bi \frac{M_{0,n}}{M'_{1,n}} \cos(n\omega t + \phi_n + \gamma_{0,n} - \gamma_{1,n}), \tag{13}$$

and the decaying contribution $\theta_{decay}(x,t)$ is

$$\theta_{decay}(x,t) = -\sum_{n=1}^{\infty} \theta_n^* \sum_{k=1}^{\infty} \beta_k(x) \times \frac{\cos(\phi_n - \operatorname{atan2}(n\omega\tau_k, 1))}{\sqrt{1 + n^2\omega^2\tau_k^2}} e^{-t/\tau_k}, \tag{14}$$

with

$$M_{0,n}e^{i\gamma_{0,n}} = \cosh(\omega''_n x')\cos(\omega''_n x') + i\sinh(\omega''_n x')\sin(\omega''_n x'), \tag{15}$$

$$\begin{aligned} M'_{1,n}e^{i\gamma_{1,n}} =& \omega''_n \sinh(\omega''_n)\cos(\omega''_n) - \omega''_n \cosh(\omega''_n)\sin(\omega''_n) \\ &+ Bi\cosh(\omega''_n)\cos(\omega''_n) + i[\omega''_n \sinh(\omega''_n)\cos(\omega''_n) \\ &+ \omega''_n \cosh(\omega''_n)\sin(\omega''_n) + Bi\sinh(\omega''_n)\sin(\omega''_n)], \end{aligned} \tag{16}$$

where

$$\omega''_n = \sqrt{\frac{n\omega H^2}{2\alpha'}}, \tag{17}$$

$$x' = \frac{x}{H}, \tag{18}$$

$$i = \sqrt{-1}, \tag{19}$$

$$Bi = \frac{hH}{k}, \tag{20}$$

$$\beta_k(x) = \frac{2\sin\hat{\lambda}_k}{\hat{\lambda}_k + \sin\hat{\lambda}_k\cos\hat{\lambda}_k}\cos\left(\hat{\lambda}_k x'\right), \tag{21}$$

where $\hat{\lambda}_k$ are the successive roots of the transcendental equation

$$\cot\hat{\lambda}_n = \frac{\hat{\lambda}_n}{Bi}, \tag{22}$$

and where

$$\tau_k = \frac{H^2}{\alpha'\hat{\lambda}_k^2}. \tag{23}$$

It is possible to combine averaged boundary conditions and pulse boundary conditions in one calculation. These calculations are called hybrid [11]. Starting from $t = 0$, the averaged heat sources are applied, and after time $t = t^*$, pulses are applied (possibly delayed by ψ). It can be shown that the temperature evolution is composed of the averaged

component $\overline{\theta}(x,t)$, a ripple $\tilde{\theta}(x,t-t^*)$ and a decaying component $\theta_{decay}(x, t-t^*)$ where the two latter start from the time $t = t^*$:

$$\theta_{hybrid}(x,t) = \overline{\theta}(x,t) + \tilde{\theta}(x,t-t^*) + \theta_{decay}(x,t-t^*). \tag{24}$$

A particularly interesting case, is when $t^* \to \infty$. The starting state at $t = t^*$ is then the averaged SS. This situation is called the Quasi Steady State ShortCut (QSSSC). When performing the QSSSC, it is convenient to start the pulsed calculation from $t = 0$, while applying the averaged SS as initial state. Note that in this case, the averaged temperature reduces to $\overline{\theta}(x,t) = \theta^*_{av}(x)$:

$$\theta_{QSSSC}(x,t) = \theta^*_{av}(x) + \tilde{\theta}(x,t) + \theta_{decay}(x,t). \tag{25}$$

When the electrode initially starts heating up, the decaying component is naturally present, cfr. Eq. 11. Using the approximative hybrid method, a significant reduction in numerical time stepping can be obtained. When we apply the hybrid calculation, and we start pulsing at $t = t^*$, the presence of the decaying component (cfr. Eqs. 24 and 25) is not natural at all. The decaying component θ_{decay} should have started already at $t = 0$, instead of at $t = t^*$, and chances are that it would have largely decayed or even totally disappeared at $t = t^*$. The presence of the decaying component $\theta_{decay}(x,t)$ troubles the approximative hybrid method, and introduces errors. Assume that at the time of interest $t = t^*$ the decaying component θ_{decay} in the full calculation would be already very small or even zero. The hybrid method would then yield good approximative results, if it would be possible to eliminate $\theta_{decay}(x, t)$ during the hybrid calculation.

The decaying component $\theta_{decay}(x, t)$ can be manipulated by delaying the pulses in time with an amount ψ. It can easily be shown that when the pulse is delayed by ψ that

$$\theta^*(t-\psi) = \sum_{n=1}^{\infty} \theta^*_n \cos(n\omega t + \phi_n - n\omega\psi) \tag{26}$$

and hence to delay the pulse by ψ, one needs to replace the phases ϕ_n by $\phi_n - n\omega\psi$ in expressions 6, 13 and 14.

The optimal value for ψ, written ψ^*, can then be calculated by minimizing $|\theta_{decay}(x, t)|$ in Eq. 14, and calculating for which ψ this occurs. This is an optimization problem. To simplify, only the component $k = 1$ is considered. This component is not necessarily the largest in amplitude, but it is always the slowest one to damp out. When the spectral content of the pulse shape is relatively low, another simplification can be done: the optimization problem can be limited to the most important spectral component. This approach is very pragmatic, but it does have the advantage that it delivers a practical closed form expression for ψ^*. This pragmatic approach proves to be very sufficient in this work. For the case of the full-wave rectified sine the major spectral component is at double frequency ($n = 2$) and the optimal pulse delay is then

$$\psi^* = \frac{1}{2\omega}\left(\frac{3\pi}{2} - \text{atan2}(2\omega\tau_1, 1)\right). \tag{27}$$

For the case of the half-wave rectified sine the major spectral component is at pulse base frequency ($n = 1$) and the optimal pulse delay is

$$\psi^* = \frac{1}{\omega}(\pi - \text{atan2}(\omega\tau_1, 1)). \tag{28}$$

For slow thermal systems, where the first and largest time constant τ_1 is very large compared to the period T, the optimal pulse delay simplifies to

$$\psi_{lim} = \lim_{\frac{T}{\tau_1}\to 0} \psi^* = \frac{T}{4}, \tag{29}$$

for both the full-wave rectified and the half-wave rectified sine.

For rectangular pulses the spectral content can be fairly large, especially when the duty cycle α becomes small. When determining ψ^* it is not justified to limit the calculation to only one spectral component. One has to consider all the spectral components that are substantially contributing. In previous work [11] an optimal pulse delay for rectangular pulses was obtained:

$$\psi^* = \tau_1 \ln\left(\alpha \frac{1 - e^{T/\tau_1}}{1 - e^{\alpha T/\tau_1}}\right). \tag{30}$$

Performing the optimization on Eq. 14 delivers the same result, but expression 30 has the advantage to be in a closed form, and is superior for practical use.

To illustrate the formulae above, some examples are shown. The temperature evolutions are calculated for a case where $x' = 0.99$, $T' = 10^{-3.8}$ and $Bi = 10^3$, where a half-wave rectified sine was applied. T' is the dimensionless period and is defined as

$$T' = \frac{\alpha' T}{H^2}. \tag{31}$$

By not delaying the pulses in time, the results from Fig. 2 are obtained. By delaying the pulses with ψ^*, the results from Fig. 3 are obtained. It can be seen that by delaying the pulses with ψ^*, $\theta_{decay}(x, t)$ during the first on-time can be reduced strongly. The time in Figs. 2 and 3 is expressed in the dimensionless time Fo, which is defined as

$$Fo = \frac{\alpha' t}{H^2}. \tag{32}$$

The impact of the undesirable $\theta_{decay}(x, t)$ will be quantified from here. Only the QSSSC will be studied. The smaller $\theta_{decay}(x, t)$, the more accurate the QSSSC

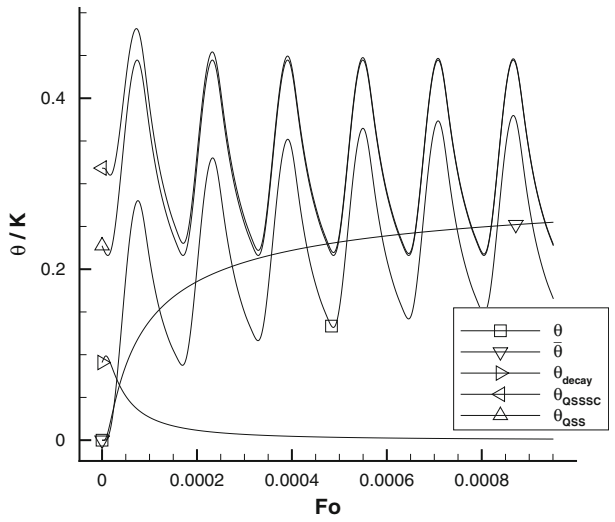

Fig. 2 Temperature evolutions in 1D slab, $\psi = 0$ (half-wave rectified sine pulses, $x' = 0.99$, $T' = 10^{-3.8}$, $Bi = 10^3$)

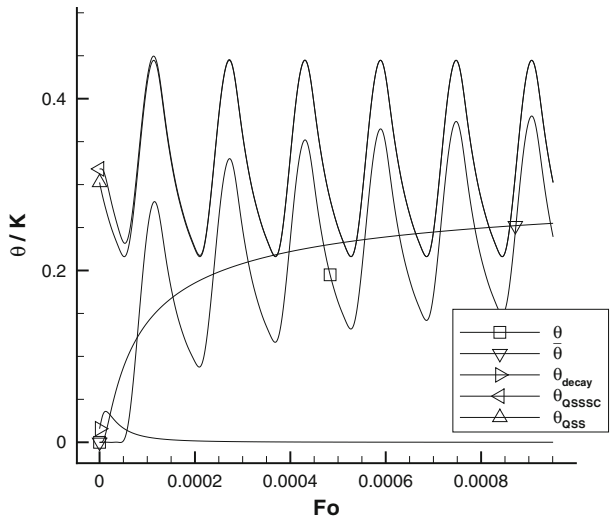

Fig. 3 Temperature evolutions in 1D slab, $\psi = \psi^*$ (half-wave rectified sine pulses, $x' = 0.99$, $T' = 10^{-3.8}$, $Bi = 10^3$)

approximates the real QSS. The difference between the QSSSC and the QSS, will be quantified with the function E (in %), which is defined as

$$E_j = \frac{\int_{\delta_j} |\theta_{QSSSC}(x,t) - \theta_{QSS}(x,t)| dt}{\int_{\delta_j} \theta_{QSS}(x,t) dt} 100 = \frac{\int_{\delta_j} |\theta_{decay}(x,t)| dt}{\int_{\delta_j} \theta_{QSS}(x,t) dt} 100, \quad (33)$$

where the integrals are calculated over δ_j, which is the jth on-time. The integration domain is limited to the on-times, because this is the only interval of interest when performing calculations for ECM. During the on-time of the pulse, the actual shape change of the workpiece occurs, which is the ultimate goal for simulations in ECM. The states during the off-times are of no primary importance. E is mainly a function of Bi, T', x' and the pulse shape. Two additional parameters are the number of on-time j, and ψ. The error during the first on-time, E_1, is shown in Fig. 4 for a half-wave rectified sine, $x' = 0.99$, with $\psi = 0$, and in Fig. 5 for the same setup, but with $\psi = \psi^*$. It can be seen that in Fig. 5 the values for E_1 are significantly lower. If the optimal pulse delay ψ^* would have been calculated using all spectral components, the zone for which $\log Bi < 0$ would be equal to zero in Fig. 5. The simplification of the calculation of ψ^* (only taking into account the one most important spectral component) leaves an error of a few percents in this case.

A more than useful amount of figures like Figs. 4 and 5 can be produced. To be able to draw a general conclusion about the errors introduced by the approximative method, the worst case values of E encountered will be summarized in a table. For a full-wave rectified sine, the worst case values can be seen in Table 1. For a half-wave rectified sine, the worst case values can be seen in Table 2.

With the full-wave rectified sine pulsing, it can be seen in Table 1 that the errors introduced by the decaying component are not very large. Delaying the pulses in time with a delay ψ^* does not dramatically reduce the error further. The pulse delaying does not have a great impact with the full-wave rectified sine pulsing. This is because of the fairly large DC component, and the first important spectral component being at double base frequency ($n = 2$), while there is a zero component at base frequency.

With the half-wave rectified sine pulsing, it can be seen in Table 2 that the worst case value of E, encountered with

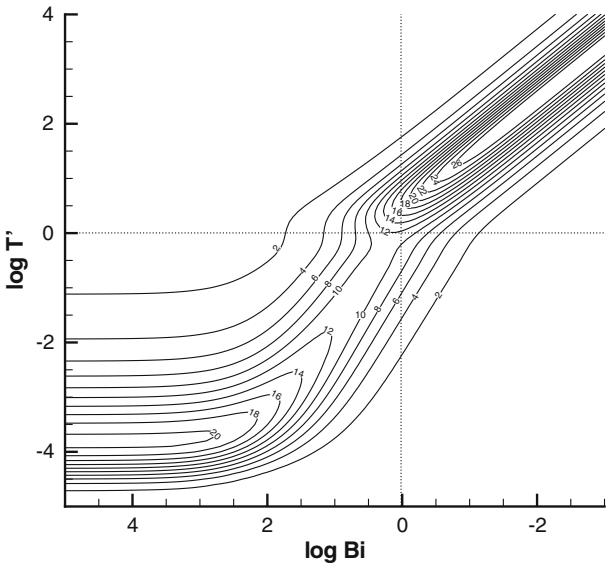

Fig. 4 E_1 as a function of Bi and T', for half-wave rectified sine pulses and $x' = 0.99$. $\psi = 0$

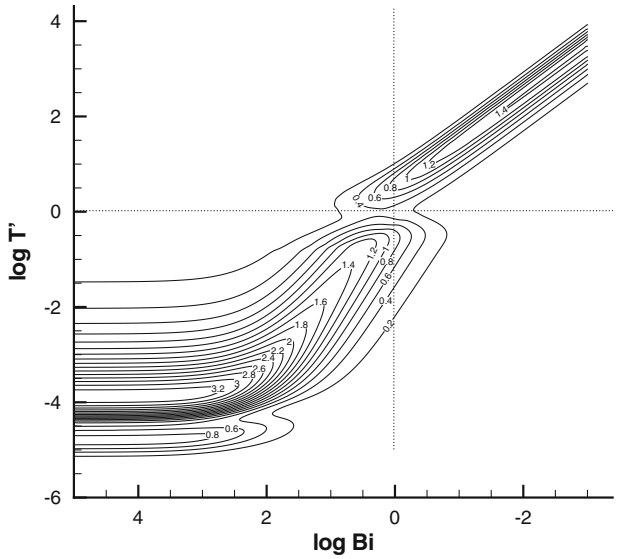

Fig. 5 E_1 as a function of Bi and T', for half-wave rectified sine pulses and $x' = 0.99$. $\psi = \psi^*$

Table 1 Full-wave rectified sine, worst case values of E

ψ	E_1 max	E_2 max
0	3.5%	0.15 %
ψ^*	1.5 %	0.05 %

Table 2 Half-wave rectified sine, worst case values of E

ψ	E_1 max	E_2 max
0	40.9%	10.4%
ψ^*	3.3%	0.5%

$\psi = 0$, is about 41%, which is not acceptable. Calculating until the second on-time during the QSSSC, we could still encounter a maximum E_2 of about 10%, which is still unacceptable. By delaying the pulses with $\psi = \psi^*$ the worst case values of E are strongly reduced. It can be seen from Table 2 that the maximum error E_1 is about 3%, which is already acceptable, since in many cases the uncertainties on the thermal parameters of the system are also of this order. Calculating until the second on-time gives a maximum E_2 of about 0.5%, which is quite satisfactory.

For rectangular pulses, the method in this work can be used to reproduce the results from former work of the authors [11]. However, due to the high spectral content of rectangular pulses, the method in this work is not ideal. For rectangular pulses specifically, the method from [11] will outperform the formulation in this work.

3.2 Convection in the electrolyte

Because in ECM the convection velocity is usually very high, convection is the main mode of transport in the electrolyte. If only convection and bulk heating is considered and the problem is reduced to 1D, Eq. 1 simplifies to a transport equation with a source

$$v\frac{\partial\theta}{\partial x} + \frac{\partial\theta}{\partial t} = \frac{P_{bulk}}{\rho C_p} = P^*(t). \tag{34}$$

The solution $\theta(x, t)$ in the flow channel is the surface tangent to the characteristic direction vector $(v, 1, P^*(t))$ in the (x, t, θ) space, according to Strauss [14]. For the full-wave rectified sine, $P^*(t)$ is defined in time as

$$P^*(t) = P^*|\sin(\omega t')|. \tag{35}$$

To provide the possibility of a pulse delay ψ, $t' = t - \psi$ is used. For the half-wave rectified sine, $P^*(t)$ is defined in time as

$$P^*(t) = \begin{cases} P^*\sin(\omega t') & \text{for } iT \le t' < (i+\frac{1}{2})T, \\ 0 & \text{for } (i+\frac{1}{2})T \le t' < (i+1)T, \end{cases} \tag{36}$$

with i the number of the period.

Other condition to obey are the initial condition $\theta(x, 0) = 0$, and the boundary condition $\theta(0, t) = 0$. Having all this information, it is possible to obtain the temperature solution in the flow channel. This solution can be shown graphically, but for brevity this is not included in this paper. In [11] the solution is shown for rectangular pulses. The solutions for a full-wave rectified sine and a half-wave rectified sine are similar. The same observations made in [11] are made with the pulse shapes in this work.

The averaged temperature evolution $\overline{\theta}(x, t)$ is calculated by choosing the source term $P^*(t)$ from Eq. 34 equal to the averaged value $\langle P^*(t) \rangle$.

When using the averaged temperature to approximate the pulsed temperature, there is a systematic underestimation during the transient accumulation of heat before the QSS is reached. If the pulses are delayed in time by $\psi = \psi_c^*$, with

$$\psi_c^* = \frac{T}{4}, \tag{37}$$

the systematic underestimation disappears, and the averaged calculation will become equal to the average temperature during the pulses. Both the full-wave rectified sine and the half-wave rectified sine yield the same ψ_c^* from Eq. 37.

When using the QSSSC to approximate the QSS, there is a systematic overestimation during the transient before the whole channel is flushed. If the pulses are delayed in time by $\psi = \psi_c^*$, the systematic overestimation disappears, and the average of the QSSSC will become equal to the average of the QSS.

Note that in the case where current pulses are applied (instead of voltage), a more accurate and still simple description of $P^*(t)$ in the electrolyte is possible. According to Eq. 2 the heat production is proportional to the square of the current density J. Hence it is more accurate to replace the $\sin(\omega t')$ in Eqs. 35 and 36 by $\sin^2(\omega t')$. This leads however to a very similar solution, and makes no difference in the obtained ψ_c^* in Eq. 37.

4 Method

If the total machining time is large enough compared to the time scales of the temperature evolution, it is a good approximation to neglect the slow transients and say that the system is always in QSS. The QSS can be computed cheaply using the QSSSC. This method is convenient for easy integration in a larger time scale time stepping calculation, for instance for the calculation of the shape change of the electrodes. Practically, first the averaged SS is calculated. Afterwards, by delaying the pulses with ψ, the QSS can be calculated in numerical calculations by time stepping through the delay interval, and the first on-time. This keeps the number of timesteps to a minimum, and should provide satisfactory predictions of temperature during the on-time. If a higher accuracy is needed, one has to time step also through the off-time, and the second on-time. For heat transfer by conduction in the electrode, an optimal delay ψ^* can be used. For the convection in the flow channel, an optimal ψ_c^* can be used. The pulse delay for convection and conduction have to be taken the same, since in the more general system they result from the same current pulsing. For $T \ll \tau_1$, $\psi^* \approx \psi_c^*$, hence applying the pulse delay is generally beneficial to the convection and the conduction case.

If the time scales of the temperature evolution are not small enough compared to the total machining time, the hybrid calculation can be used. This method is analogous to the QSSSC above, except that the initial state before applying the pulses is obtained by time stepping (with large timesteps). Delaying the pulse on-time is advantageous to minimize $\theta_{decay}(x,t)$ and calculating more periods will provide more accurate results. The worst case errors are not quantified in this case, and will be higher than with the QSSSC.

5 Conclusions

As a general method to solve thermal problems during PECM, the full transient calculation is always an option. However, this method can be computationally very expensive, if not practically impossible, if the full detail of the pulses has to be considered. When the full transient calculation would be too expensive, simplified methods are proposed: the hybrid calculation and the QSSSC. The approximative methods can be performed with a minimum of computational effort.

Analytical solutions of simplified sub-problems were analyzed in this work. The assumptions of the models, used to derive the analytical solutions, are too strict for real life Electrochemical Machining (ECM) conditions. Nevertheless, interesting conclusions can be made.

The analysis is performed for a full-wave rectified sine and a half-wave rectified sine pulsing. With the spectral formulation in this work any pulse shape can be investigated. Analytical expressions for optimal values of ψ are obtained in this work. Applying these time delays ψ to the pulses during the calculations strongly improves the results of the approximative methods.

References

1. Lohrengel M, Klueppel I, Rosenkranz C, Betterman H, Schultze J (2003) Microscopic investigations of electrochemical machining of Fe in $NaNO_3$. Electrochim Acta 48(20–22):3203–3211
2. Mount A, Clifton D, Howarth P, Sherlock A (2003) An integrated strategy for materials characterisation and process simulation in electrochemical machining. J Mater Process Technol 138:449–454
3. Rajurkar KP, Zhu D, McGeough JA, Kozak J, De Silva A (1999) New developments in electro-chemical machining. Ann CIRP 48(2):567–579
4. Kozak J, Rajurkar K (1991) Computer simulation of pulse electrochemical machining (PECM). J Mater Process Technol 28(1–2):149–157
5. Kozak J (2004) Thermal models of pulse electrochemical machining. Bull Pol Acad Sci: Tech Sci 52(4):313–320
6. Datta M, Landolt D (1981) Electrochemical machining under pulsed current conditions. Electrochim Acta 26(7):899–907
7. Kozak J, Rajurkar K, Lubkowski K (1997) The study of thermal limitation of electrochemical machining process. Trans NAMRI/SME XXV, 159–164
8. Clark W, McGeough J (1977) Temperature distribution along the gap in electrochemical machining. J Appl Electrochem 7:277–286
9. Loutrel S, Cook N (1973) A theoretical model for high rate electrochemical machining. ASME J Eng Ind 95(B/4):1003–1008
10. Smets N, Van Damme S, De Wilde D, Weyns G, Deconinck J (2007) Calculation of temperature transients in pulse electrochemical machining. J Appl Electrochem 37(3):315–324
11. Smets N, Van Damme S, De Wilde D, Weyns G, Deconinck J (2007) Time averaged temperature calculations in pulse electrochemical machining, part I: theoretical basis. J Appl Electrochem 37(11):1345–1355
12. Smets N, Van Damme S, De Wilde D, Weyns G, Deconinck J (2008) Time averaged temperature calculations in pulse electrochemical machining, part II: numerical simulations. J Appl Electrochem 38(4):551–560
13. Carslaw HS, Jaeger JC (1959) Conduction of heat in solids. Oxford University Press, New York.
14. Strauss W (1992) Partial differential equations: an introduction. Wiley, New York